Jordanian Journal of Computers and Information Technology (JJCIT), Vol. 08, No. 02, June 2022.

BANDWIDTH ENHANCEMENTS AND SIZE REDUCTION OF 3 DB PATCH COUPLER WITH 45° OUTPUT PHASE DIFFERENCE FOR 5G BEAMFORMING NETWORKS

Nazleen S. M. Suhaimi, Anthony N. Uwaechia and Nor M. Mahyuddin

(Received: 23-Jan.-2022, Revised: 14-Mar.-2022, Accepted: 6-Apr.-2022)

ABSTRACT

In this article, a single-layered 3 dB/45° coupler (Design D) is proposed for fifth-generation (5G) beamforming networks using cross-slotted patch topology, dumbbell-shaped slots, loaded stubs, notches and rectangular ground slots. The proposed Design D coupler is capable of eliminating the need for additional 45° phase shifters in the beamforming networks such as Butler matrix, which provides the main contribution in this work, especially in size reduction and bandwidth enhancements. The fractional bandwidths of 28.90%, 39.14% and 35.91% for -10 dB of $|S_{11}|$, -3 dB ± 1 dB of $|S_{31}|$ and 5° phase imbalance of output phase difference are achieved by the proposed Design D coupler. The bandwidth enhancements of -3 dB ± 1 dB coupling coefficient, S_{31} and 45° ± 5° output phase difference for the proposed Design D coupler are 22.52% and 23.14% compared to Design A coupler, respectively. The bandwidth of 45° ± 5° output phase difference is increased by 16.3% owing to the presence of rectangular ground slots in Design D compared to Design C coupler. The patch size of the proposed Design D coupler is 0.22 λ_g x 0.23 λ_g. The electrical size of the proposed Design D coupler is reduced by 45.72% compared to Design A coupler.

KEYWORDS

5G beamforming networks, Patch coupler, Output phase difference, Bandwidth enhancement, Size reduction.

1. INTRODUCTION

As a pioneer in fifth-generation (5G) wireless communication, the 6 GHz band is currently allocated in many countries [1]-[2]. A good trade-off between equipment size, network coverage and ubiquitous high-speed connectivity in all locations becomes a remarkable challenge for researchers and engineers involved in the development of radio frequency (RF) and microwave components, antenna design and network planning.

Passive microwave couplers are the main components found in beamforming networks such as Butler matrix [3]-[7], Blass matrix [8]-[11] and Nolen matrix [12]-[13]. Branch-line couplers are extensively utilized in beamforming networks to provide an equal 3 dB power split with a standard 90° output phase difference within the desired frequency band [14]. Nevertheless, the traditional branch-line couplers provide large size and narrow bandwidth. The restricted standard 90° output phase difference between the output signals of the traditional branch-line coupler further restricts its applications. The reported improvements in the branch-line coupler performance mainly focus on multiband [15]-[19], arbitrary power division ratio [20]-[21], broadband [22]-[24], compact size [25] and integration with additional phase shifter [26]-[27]. The traditional couplers can provide output phase differences of 0°, 90° and 180°, but the non-standard phase difference such as 30°, 45° or 150° could not be realized without additional phase shifters. Nowadays, the non-standard phase characteristic coupler is being potentially highly demanded in smart antenna systems, measurement tools and power amplifiers. The most straightforward method to solve this problem is to propose additional phase shifters, but they contribute major drawbacks, such as large circuit size and inevitable large insertion loss between main line and reference line. The unequal insertion loss is further aggravated through the final stage of a feed network causing intolerable magnitude fluctuations among other output ports. Although bandwidths of the phase shifters in [28]-[30] are enhanced, these works are undesirable for low-cost applications due to high fabrication complexities.

As a step towards 5G technology, there is extremely high demand for a wideband operation, compact in size and low cost in modern microwave circuits. Therefore, the coupler structure which can provide any non-standard output phase difference without any additional phase shifter circuit quickly draws

N. S. M. Suhaimi, A. N. Uwaechia and N. M. Mahyuddin are with School of Electrical and Electronic Engineering, Universiti Sains Malaysia, Penang, Malaysia. Emails: nsyahira@student.usm.my, anthony_uwaechia@usm.my and eemnmuzlifah@usm.my

attention. Furthermore, an effective approach to achieve impedance matching and phase stabilization is desired. The previous branch-line couplers have output phase difference of 90° and other output phase differences could only be realized using additional phase shifters. This increased circuit size and cost as well as degraded the overall performances owing to interconnecting mismatch losses.

Nowadays, Butler matrix is one of the most popular realizations of the beamforming network. Nevertheless, the required output phase differences found in the Butler matrix are 45° and 135°, which cannot be realized with the traditional power divider or branch-line coupler without using additional phase shifters. In order to circumvent the arising issues, the proposed 3 dB patch coupler with 45° output phase difference is capable of eliminating the need for additional 45° phase shifters, which provides the main contribution in this work, especially in size reduction and bandwidth enhancements of S-parameter responses and output phase difference.

In this work, a single-layered 3 dB patch coupler with 45° output phase difference is proposed without using any phase shifter. The bandwidth performance of the desired phase difference for the proposed 3 dB/45° patch coupler can be controlled by selecting the suitable dimensional lengths and widths of the dumbbell-shaped slots, whilst the bandwidth performances of the reflection and coupling coefficients are controlled by the dimensional lengths and widths of the cross slots and loaded stubs. By comparing the couplers in [31-33], the bandwidth performances of reflection and coupling coefficients are controlled by impedances of transmission lines, whilst the output phase difference is controlled by the electrical lengths of the transmission lines.

Conventionally, the traditional 4 × 4 Butler matrix comprises four traditional 3 dB/90° branch-line couplers, two traditional 0 dB crossovers, two 0° phase shifters and two 45° phase shifters. Meanwhile, the physical size of 4 × 4 Butler matrix can be reduced using two proposed 3 dB/90° patch couplers (Design B) with a size reduction of 26.32% and two proposed 3 dB/45° patch couplers (Design D) with a size reduction of 45.72% compared to their traditional designs. The Butler matrix can be realized without using any phase shifters and crossovers as reported in [34], thereby making it remarkably of low transmission loss, low insertion loss, less number of components and more compact compared to the traditional Butler matrix. The patch topology is adopted from [35], where the inductive loading effect of cross slots results in a significant size reduction. The parametric analyses are carried out on the designed couplers to analyse the effects of cross slots' and stubs' length variations on the S-parameter bandwidth performances. Moreover, the power division ratio and output phase difference performances are investigated and analyzed. The 90° output phase difference is reduced to 45° by introducing the dumbbell-shaped slots at the end of the cross slots as well as optimizing the lengths and widths of the cross slots and rectangular stubs. Meanwhile, the chamfering corners are optimized to readjust the impedance matching to 50 Ω. Notches are placed along each length and width of the patch to ensure the minimum resonant amplitudes of reflection coefficient, $|S_{11}|$ and isolation, $|S_{41}|$ at the center frequency of 6.5 GHz.

Slotlines in the ground plane introduce a slow wave structure, where the phase velocity of the propagating wave is smaller than the velocity of light. This makes a slotted ground plane become electrically longer. Since any additional phase shifter is not required in this work, this approach makes the proposed design different from the work reported in [26-27] and provides the main contribution in this work, especially in terms of bandwidth enhancements and size reduction.

The proposed 3 dB/45° patch coupler can operate at the center frequency of 6.5 GHz which is suitable for unlicensed used in 5.9 GHz to 7.1 GHz band that meets 5G spectrum requirements as supported by Federal Communications Commission (FCC) [2]. The proposed 3 dB/45° patch coupler is designed using Computer Simulation Technology (CST) Microwave Studio software as well as fabricated onto Rogers RO4003C board with substrate thickness, h of 0.813 mm and dielectric constant, ε_r of 3.38.

2. DESIGN ANALYSIS

Theoretically, power entering port 1 of the traditional 3 dB branch-line coupler is equally split between output ports, where the coupling factor is 3 dB with a 90° output phase difference. No power is coupled to the isolated port with all ports matched. The physical layout of the traditional 3 dB branch-line coupler with 90° output phase difference is depicted in Figure 1.

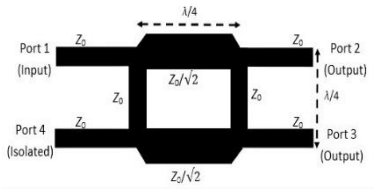

Figure 1. Physical layout of traditional 3 dB branch-line structure with 90° nominal electrical length [36].

A block diagram of the traditional 3 dB branch-line coupler with an additional 45° phase shifter and the proposed 3 dB coupler without any additional phase shifter is illustrated in Figure 2 (a). The phase difference of the traditional 45° phase shifter can be determined by using the following expression [37]:

$$\text{Phase difference, } \Delta\phi = \frac{2\pi\,(L_m - L_r)}{\lambda_g} \quad (1)$$

where L_m, L_r and λ_g are the main length, reference length and guide wavelength, accordingly. The calculated L_m is 17.73 mm and has been optimized to obtain the desired 45° phase difference between the output ports (port 2 and port 3). The traditional 3 dB/90° branch-line coupler is combined with the traditional 45° phase shifter to develop 3 dB coupling value and 45° output phase difference. According to Equation (1), the electrical length of the main line will affect the value of the output phase difference. Figure 2 (b) shows that the 45° output phase difference for combination of the traditional 3 dB coupler with 45° phase shifter is calculated as $((\theta_{ab} + \theta_{be}) - (\theta_{ad} - \theta_{df}))$, when an input signal is excited at port 1. Meanwhile, the 45° output phase difference of the proposed 3 dB coupler without phase shifter is calculated as $((\theta_{a'b'}) - (\theta_{a'd'}))$, when an input signal is excited at port 1.

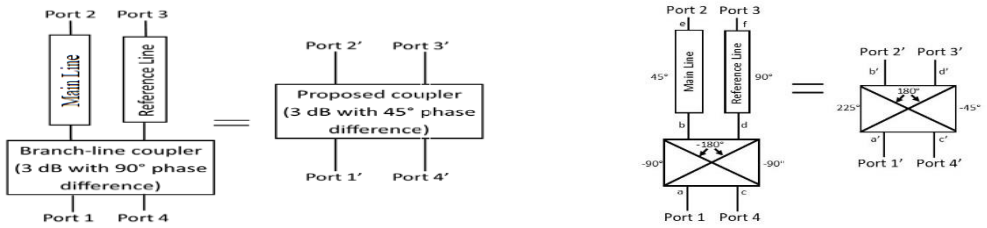

(a) (b)

Figure 2. Traditional 3 dB coupler with 45° phase shifter and proposed equivalent: (a) Block diagram; (b) Signal paths.

The physical layout of the traditional 3 dB branch-line coupler with 45° phase shifter (Design A) is depicted in Figure 3. The parameters of Design A coupler are listed in Table 1. The objective of this work is to construct a single-layered 3 dB patch coupler with 45° output phase difference without using any phase shifter, which provides bandwidth enhancements and size reduction characteristics.

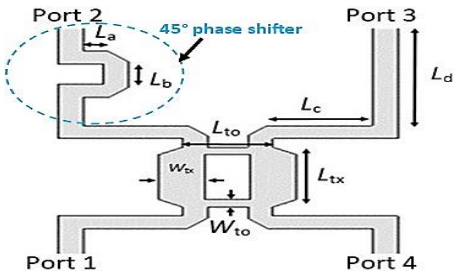

Figure 3. Physical layout of traditional 3 dB branch-line coupler with 45° phase shifter (Design A).

Table 1. Parameters of Design A coupler.

Parameters	Values (mm)
L_{to}	6.65
L_{tx}	7.45
L_a	1.46
L_b	2.91

L_c	7.3
L_d	14.59
W_{to}	1.02
W_{tx}	3.4

The proposed 3 dB/45° patch coupler (Design C) is implemented by modifying the 3 dB/90° patch coupler (Design B). The physical topology and photograph of Design B coupler under test are shown in Figure 4 (a) and Figure 4 (b), respectively.

(a) (b)

Figure 4. 3 dB/90° patch coupler with loaded stubs (Design B): (a) Physical topology; (b) Photograph under test.

Initially, the 3 dB/90° patch coupler is implemented by constructing a pair of cross slots on the square patch of the 3 dB/90° coupler (Design B). The cross slots are developed diagonally on the square patch to perturb the original patch resonator. Four feeding ports are placed in the middle of the square patch sides and matched to a characteristic impedance, Z_o which corresponds to 50 Ω. Each feeding port in Design B coupler is bent and extended to adapt with 0.5 λ_o inter-element spacing of the patch antenna array that can be integrated with Design B coupler to develop a switched-beam Butler matrix. The dimensions of length, L_t and width, W_t for the microstrip feeding ports can be calculated by substituting the dielectric method [31]. The calculated L_t equals a quarter-wavelength, whilst the calculated W_t is 1.88 mm. The dimensions of L_t and W_t are optimized to provide the optimum performance results. The initial widths of the cross slots, W_1 and W_2 are set to the available minimum fabrication limit of 0.2 mm. The capacitance and mismatch loss are reduced by chamfering each corner of the patch coupler. The initial lengths of the cross slots, L_1 and L_2 can be calculated using the Pythagorean theorem formula. Some parameters of the cross slots such as L_1, L_2, L_t, W_1 and W_2 are optimized to reroute the electric currents around the cross slots. According to the physical limitation of the square patch dimension, L_1 and L_2 are set to be less than R = 9.98 mm. Since it is not easy to convert the patch resonator into an analytical transmission line model, the physical layout is divided into four zones by the dash lines, as depicted in Figure 5. Each zone with different colours can be approximately corresponded to its equivalent transmission line model of the traditional branch-line coupler.

(a) (b)

Figure 5. Schematic relationship: (a) Traditional branch-line hybrid coupler; (b) Cross-slotted patch coupler.

By applying the even-odd mode analyses [38]-[39], the transmission (T) and reflection coefficients (Γ) are obtained for each half circuit and the overall vector amplitudes of the signals emerging from the even-odd mode reflection and transmission coefficients could be determined as follows:

$$S_{11} = \frac{\Gamma_e + \Gamma_o}{2} \quad (2)$$

$$S_{21} = \frac{T_e + T_o}{2} \quad (3)$$

$$S_{31} = \frac{T_e - T_o}{2} \quad (4)$$

$$S_{41} = \frac{\Gamma_e - \Gamma_o}{2} \quad (5)$$

The relationships between even-odd mode transmission coefficient equal to minus the odd-mode transmission coefficient are summarized in Equations (6)-(9). The phase difference between output ports is denoted by ψ.

$$S_{11} = S_{41} = 0 \quad (6)$$

$$S_{21} = T_e \quad (7)$$

$$S_{41} = \Gamma_e \quad (8)$$

$$\frac{S_{21}}{S_{31}} = \frac{\sqrt{(1-C^2)}}{C} e^{j\psi} \quad (9)$$

As ψ is defined between 0° and 90° to meet the arbitrary phase difference, the closed-form design equations can be further simplified as:

$$Z_1 = Z_0 \frac{\sqrt{(1-C^2)}}{C} \sin\psi \quad (10)$$

$$Z_2 = Z_0 \sin\psi \sqrt{\frac{(1-C^2)}{C^2+\sin^2\psi\,(1-C^2)}} \quad (11)$$

$$Z_3 = Z_2 \quad (12)$$

$$\theta_1 = 90° \quad (13)$$

$$\theta_2 = \cos^{-1}\left[-\sqrt{(1-C^2)}\cos\psi\right] \quad (14)$$

$$\theta_3 = 180° - \theta_2 \quad (15)$$

$$Z_2 = Z_0 \sin\psi \sqrt{\frac{(1-C^2)}{C^2+\sin^2\psi\,(1-C^2)}} \quad (16)$$

$$Z_3 = Z_2 \quad (17)$$

$$\theta_1 = 90° \quad (18)$$

$$\theta_2 = \cos^{-1}\left[-\sqrt{(1-C^2)}\cos\psi\right] \quad (19)$$

$$\theta_3 = 180° - \theta_2 \quad (20)$$

ψ = 90° in both Design A and Design B couplers, whilst the calculated Z_1 = 50 Ω, Z_2 = Z_3 = 35.36 Ω and $\theta_1 = \theta_2 = \theta_3$ = 90°. Nevertheless, it is difficult to realize the equivalent closed-form transmission line theory owing to the complicated field distribution on the cross-slot patch, as discussed in [40]. However, this can be achieved by adjusting the length and width of the inductive slots. Theoretically, the series inductance of the microstrip line is reduced, while the shunt capacitance is increased after converting the layout from the microstrip line into the patch structure. The cross slots' lengths, such as L_1 and L_2, are optimized to make the minimum frequencies of $|S_{11}|$ and $|S_{41}|$ be similar at 6.5 GHz.

Next, rectangular stubs are introduced at each feeding port to improve the bandwidth of S-parameter responses. The lengths of cross slots and stubs vary inversely with the frequency of propagation according to Equation (21) [31]. The square patch occupies an area of 0.2 λ_o × 0.2 λ_o. The final dimensions of Design B coupler are listed in Table 2. Design B coupler achieves a size reduction of 26.32% compared to the traditional 3 dB branch-line coupler.

$$\text{Frequency} = \text{Propagation velocity / wavelength} = v/(\lambda\sqrt{(\varepsilon\_r)}) \quad (21)$$

Table 2. Final dimensions of Design B coupler.

Parameters	Values (mm)	Parameters	Values (mm)
L_t	9.39	L_{s2}	4.53
L_1	9.85	W_t	1.84
L_2	5.92	W_1	0.80
L_c	6.65	W_2	0.60
L_d	4.00	W_s	0.30
L_{s1}	5.00		

After that, the design topology of Design B coupler in Figure 4 (a) has been modified to implement the proposed 3 dB patch coupler with 45° output phase difference without using 45° phase shifter (Design C). The design modification is realized by reducing the output phase difference from 90° to 45°. ψ is

set to 45°, whilst the calculated $Z_1 = 35.36\ \Omega$, $Z_2 = Z_3 = 27.36\ \Omega$, $\theta_1 = 90°$, $\theta_2 = 120°$ and $\theta_3 = 60°$ using Equations (10)-(20). The design modification steps for the proposed 3 dB/45° patch coupler are realized as follows:

i. Dumbbell-shaped slots are introduced at the end of the cross slots, whilst lengths and widths of the patch, cross slots and rectangular stubs are optimized to reduce the output phase difference from 90° to 45°. The desired phase difference is controlled by selecting the suitable length and width of the dumbbell-shaped slots.

ii. The microstrip line is readjusted back to 50 Ω by optimizing the dimensions of chamfering corners while maintaining the performance of -10 dB reflection coefficient, $|S_{11}|$.

iii. Notches are placed along each length and width of the patch coupler by adopting the inset feeding technique to electrically tune the resonant amplitudes of reflection coefficient, $|S_{11}|$ and isolation, $|S_{41}|$ at the center frequency of 6.5 GHz as well as to improve the -3 dB ± 1 dB transmission coefficient, $|S_{21}|$.

iv. Rectangular slots are loaded at the ground plane (Design D) to improve the bandwidths of 45° ± 5° phase imbalance, -3 dB ± 1 dB transmission coefficient, $|S_{21}|$ and -3 dB ± 1 dB coupling coefficient, $|S_{31}|$.

The physical topologies of 3 dB/45° patch coupler without rectangular ground slot (Design C) and 3 dB/45° patch coupler with rectangular ground slots (Design D) are illustrated in Figure 6 (a) and Figure 6 (b), respectively. The photograph of the proposed Design D coupler with the rectangular ground slots under test is depicted in Figure 7. The final dimensions of Design C and Design D couplers are listed in Table 3. The proposed Design D coupler occupies an area of 0.22 λ_0 × 0.23 λ_0, which contributes to a size reduction of 45.72% compared to Design A coupler.

This proposed work is recommended for the beamforming network such as Butler matrix without using any additional phase shifter, which contributes to overall size reduction. The miniaturization factor (MF) for the proposed 3 dB/45° patch coupler with rectangular ground slots (Design D) can be calculated using the following equation:

$$\text{MF}\ (\%) = \frac{A_{\text{traditional}} - A_{\text{proposed}}}{A_{\text{traditional}}} \times 100 \qquad (22)$$

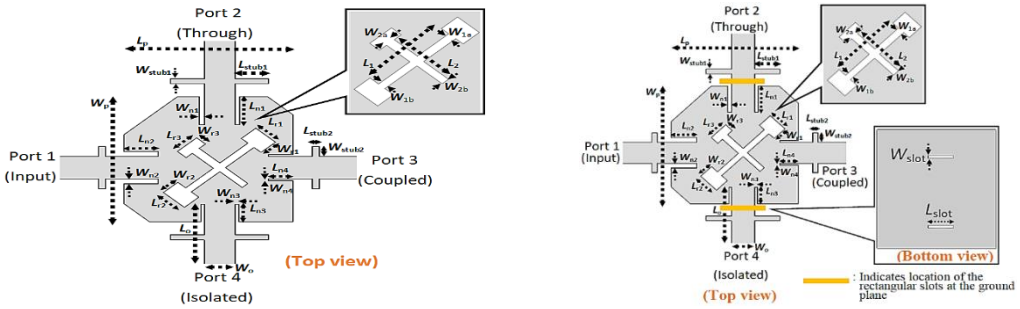

(a) (b)

Figure 6. Physical layout of 3 dB patch couplers with 45° output phase difference: (a) Without rectangular ground slots (Design C); (b) With rectangular ground slots (proposed Design D).

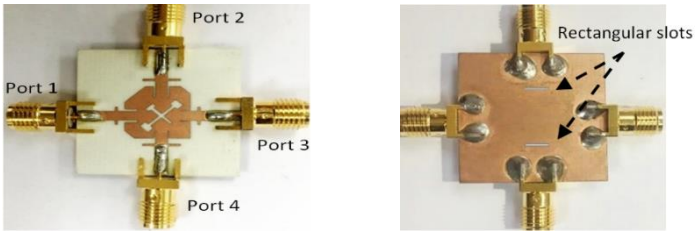

(a) (b)

Figure 7. Photograph of fabricated Design D coupler with rectangular ground slots (proposed): (a) Top view; (b) Bottom view.

Table 3. Final dimensions of Design C and Design D couplers.

Parameters	Design C coupler	Design D coupler (proposed)
	Values (mm)	Values (mm)
L_o	7.50	
L_p	10.12	
L_1	5.31	
L_2	4.14	
L_{r1}	1.65	
L_{r2}	1.78	
L_{r3}	1.64	
L_{stub1}	2.02	
L_{stub2}	0.41	
L_{n1}	2.36	
L_{n2}	2.06	
L_{n3}	1.48	
L_{n4}	1.51	
L_{slot}	-	3.98
W_o	1.84	
W_p	10.50	
W_{r1}	1.22	
W_{r2}	1.20	
W_{r3}	0.73	
W_{1a}	0.51	
W_{1b}	0.50	
W_{2a}	0.59	
W_{2b}	0.48	
W_{stub1}	0.41	
W_{stub2}	0.88	
W_{n1}	0.29	
W_{n2}	0.42	
W_{n3}	0.20	
W_{n4}	0.20	
W_{slot}	-	0.38

3. RESULTS AND DISCUSSION

As observed in Figure 8, the -10 dB fractional bandwidths of the return loss, $|S_{11}|$ and isolation, $|S_{41}|$ for the integration of 3 dB branch-line coupler and 45° phase shifter (Design A) are 14.15% and 34.3% in simulation, whilst 10.77% and 23.07% in measurement, respectively. Meanwhile, the -3 dB ± 1 dB bandwidths of the respective transmission coefficient, $|S_{21}|$ and coupling, $|S_{31}|$ are 25.08% and 16.62% in simulation, whereas 23.07% and 16% in measurement. The 5° phase fluctuation bandwidths of the simulated and measured output phase differences are 12.77% and 13.23%, respectively. At the center frequency of 6.5 GHz, the simulated $|S_{11}|$ for Design A coupler is -13.59 dB, whereas the simulated $|S_{41}|$ is -15.3 dB. Both measured $|S_{11}|$ and $|S_{41}|$ are -18.23 dB and -14.38 dB, respectively. Meanwhile, the simulated $|S_{21}|$ is -3.31 dB, whereas the measured $|S_{21}|$ is -3.07 dB. Both simulated and measured $|S_{31}|$ are -3.71 dB and -3.93 dB, individually. The output phase difference is 45.45° in simulation, whereas 47.45° in measurement.

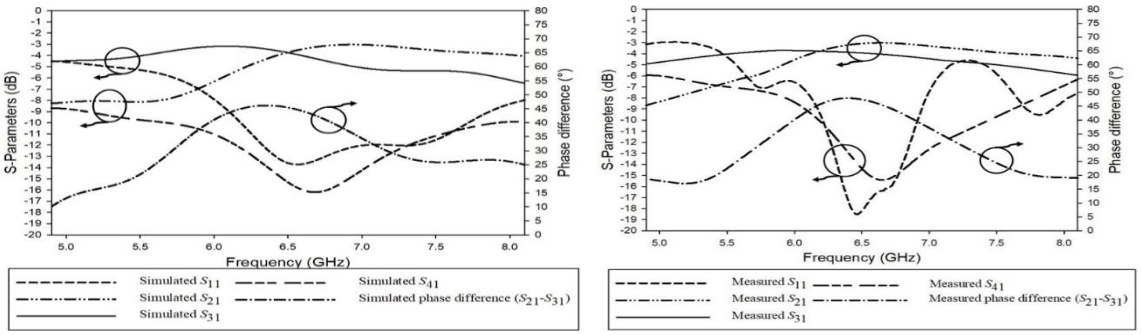

(a) (b)

Figure 8. Integration of conventional 3 dB/90° branch-line coupler and 45° phase shifter (Design A): (a) Simulation results; (b) Measurement results.

Figure 9 shows the parametric analyses of variation cross slot's length, L_1 before loading the stubs and stub's length, L_{s1} after loading the stubs in Design B coupler. Figure 9 (a) shows that the values of the minimum peak for the matching response of $|S_{11}|$ are decreased and the operating frequency is shifted to the right by decreasing L_1. Although L_{s1} equals 3 mm, as shown in Figure 9 (b), provides the highest bandwidth of the 90° ± 5° differential output phase, L_{s1} equals 5 mm is chosen in Design C, because it provides the highest fractional bandwidths of the simulated $|S_{11}|$, $|S_{21}|$, $|S_{31}|$ and $|S_{41}|$ compared to the other lengths of L_{s1}, as stated in Table 4.

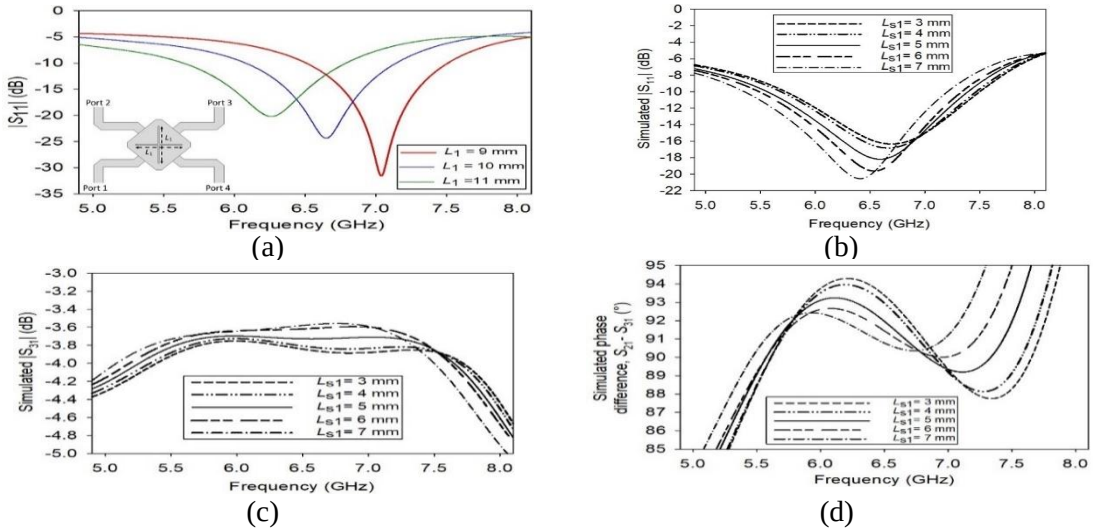

Figure 9. Parametric analyses of Design B coupler: (a) Simulated $|S_{11}|$ for the variation of cross slot's length, L_1; (b) Simulated $|S_{11}|$ for the variation of stub's length, L_{s1}; (c) Simulated $|S_{31}|$ for the variation of stub's length, L_{s1}; (d) Simulated phase difference, $|S_{21}|$ - $|S_{31}|$ for the variation of stub's length, L_{s1}.

Table 4. Summarization of the proposed 3 dB/90° cross-slotted patch coupler with loaded rectangular stubs (Design C) performances based on the variations of stubs' lengths.

Variations of stub's lengths, L_{s1} (mm)	**Bandwidth performance**				
	$\|S_{11}\| \leq$ -10 dB	**$\|S_{21}\|$ = -3 ± 1 dB**	**$\|S_{31}\|$ = -3 ± 1 dB**	**$\|S_{41}\| \leq$ -10 dB**	**Phase difference = 90° ± 5°**
3	24.15	18.77	35.85	38.92	39.54
4	27.23	18.15	36.15	39.69	38.92
5	28.00	19.85	36.46	40.92	37.84
6	27.84	18.77	36.00	40.76	35.08
7	28.00	19.08	36.15	39.38	33.85

The simulation and measurement results of S-parameters and output phase difference for the 3 dB/90° patch coupler with loaded stubs (Design B) are depicted in Figure 10. The -10 dB fractional bandwidths of the return loss, $|S_{11}|$ and isolation, $|S_{41}|$ for Design B coupler are 28% and 40.92% in simulation, whilst 30% and 36% in measurement, respectively. Meanwhile, the -3 dB ± 1 dB bandwidths of the respective transmission coefficient, $|S_{21}|$ and coupling, $|S_{31}|$ are 19.85% and 36.46% in simulation, whereas 18.46% and 34.77% in measurement. The 5° phase fluctuation bandwidths of the simulated and measured output phase differences are 37.84% and 38.62%, respectively. At 6.5 GHz, the simulated $|S_{11}|$ is -17.43 dB, whereas the simulated $|S_{41}|$ is -18.37 dB. Both measured $|S_{11}|$ and $|S_{41}|$ are -16.41 dB and -16.68 dB, respectively. Meanwhile, the simulated $|S_{21}|$ is -3.17 dB, whereas the measured $|S_{21}|$ is -3.32 dB. Both simulated and measured $|S_{31}|$ are -3.84 dB and -3.54 dB, individually. The output phase difference at 6.5 GHz is 90.82° in simulation, whereas 89.83° in measurement.

Figure 11 shows the simulation results of S-parameters and output phase difference for the 3 dB/45° patch coupler by applying step 1 to step 2 (Design C). The -10 dB fractional bandwidths of the simulated $|S_{11}|$ and $|S_{41}|$ for Design C coupler are 19.23% and 49.23%, respectively. The 1 dB amplitude fluctuation bandwidth for the simulated $|S_{21}|$ is 10.31%, whilst 35.07% for the simulated $|S_{31}|$. As observed, the

output phase difference of Design C coupler is capable to reduce from 90° to 45°. However, the bandwidth of $|S_{21}|$ is less than 18.5%. The bandwidth of 5° phase imbalance for the simulated output phase difference is 36.15%. At 6.5 GHz, the simulated $|S_{11}|$ is -18.76 dB, whereas the simulated $|S_{41}|$ is -19.73 dB. The simulated $|S_{21}|$ is -3.87 dB, whereas the simulated $|S_{31}|$ is -2.85 dB. Meanwhile, the simulated output phase difference at 6.5 GHz is 48.37° with a phase deviation of 1.63°.

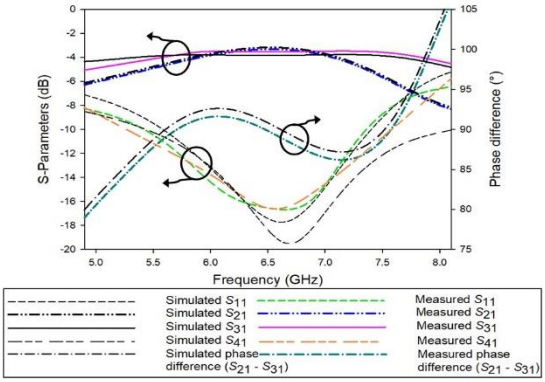

Figure 10. Simulation and measurement results of S-parameters and output phase difference for the 3dB/90° patch coupler with loaded stubs (Design B).

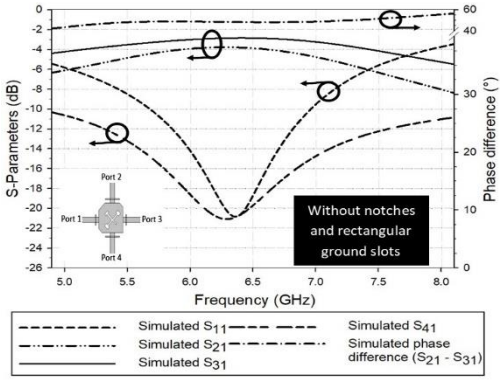

Figure 11. Simulation and measurement results of S-parameters and output phase difference for the 3dB/45° patch coupler by applying step 1 to step 2 (Design C).

Figure 12 shows the simulation results of S-parameters and output phase difference for the 3 dB/45° patch coupler by applying step 1 to step 3 (Design C). The -10 dB fractional bandwidths of the simulated $|S_{11}|$ and $|S_{41}|$ for Design C coupler are 26.02% and 47.07%, respectively. The 1 dB amplitude fluctuation bandwidth for the simulated $|S_{21}|$ is 23.69%, whilst 33.90% for the simulated $|S_{31}|$. As observed, the output phase difference of Design C coupler is capable to reduce from 90° to 45° without interfering with the performance of -3 dB coupling coefficient, maintaining the patch size by doing this modification. The bandwidth of 5° phase imbalance for the simulated output phase difference is 19.61%. At 6.5 GHz, the simulated $|S_{11}|$ is -32.37 dB, whereas the simulated $|S_{41}|$ is -28.86 dB. The simulated $|S_{21}|$ is -3.17 dB, whereas the simulated $|S_{31}|$ is -3.29 dB. Meanwhile, the simulated output phase difference at 6.5 GHz is 49.43° with a phase deviation of 4.43°. As observed, the presence of notches increases the -10 dB fractional bandwidth of the simulated $|S_{11}|$ and 1 dB amplitude fluctuation bandwidth for the simulated $|S_{21}|$. Moreover, the resonant amplitudes of reflection coefficient, $|S_{11}|$ and isolation, $|S_{41}|$ are electrically tuned at the center frequency of 6.5 GHz.

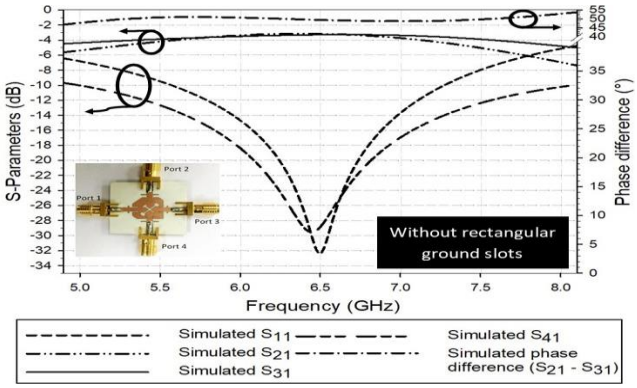

Figure 12. Simulation and measurement results of S-parameters and output phase difference for the 3dB/45° patch coupler by applying step 1 to step 3 (Design C).

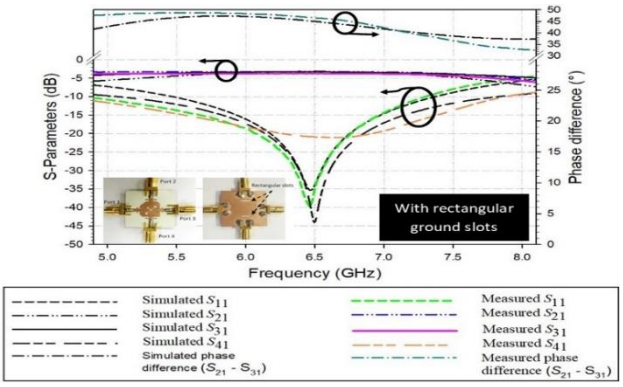

Figure 13. Simulation and measurement results of S-parameters and output phase difference for the proposed 3 dB/45° patch coupler by applying step1 to step 4 (Design D).

In order to improve the bandwidth performances of S-parameters and output phase difference from Design C coupler (without rectangular ground slots), rectangular ground slots are introduced in Design

D coupler. As observed, Figure 13 illustrates that the -10 dB fractional bandwidths of $|S_{11}|$ and $|S_{41}|$ for Design D coupler are 28.90% and 42.31% in simulation, whilst 37.08% and 46% in measurement. The respective -3 dB ± 1 dB bandwidths of $|S_{21}|$ and $|S_{31}|$ are 24.62% and 39.14% in simulation, whereas 42% and 37.08% in measurement. The output phase difference is 45° ± 5° between 4.9 GHz and 7.23 GHz which corresponds to 35.91% in simulation, whereas between 4.9 GHz and 7.18 GHz which corresponds to 35.08% in measurement. At 6.5 GHz, the simulated $|S_{11}|$ is -31.89 dB, whereas the simulated $|S_{41}|$ is -38.55 dB. Both measured $|S_{11}|$ and $|S_{41}|$ are -35 dB and -20.99 dB, respectively. The simulated $|S_{21}|$ is -3.17 dB, whereas the measured $|S_{21}|$ is -3.21 dB. Meanwhile, $|S_{31}|$ is -3.28 dB in simulation, whereas -3.71 dB in measurement.

The simulated output phase difference at 6.5 GHz is 45° without phase deviation, whereas the measured output phase difference is 46.62° with a phase deviation of ± 1.62°. The tolerances of measurement results are caused by the junction discontinuities as well as inaccuracy of measurement instrument and fabrication. The bandwidth enhancements of -3 dB ± 1 dB coupling coefficient, $|S_{31}|$ and 45° ± 5° output phase difference for Design D coupler are 22.52% and 23.14% compared to Design A coupler, respectively. Meanwhile, the bandwidth of the output phase difference in Design D coupler is improved by 16.3% owing to the presence of rectangular ground slots compared to Design C coupler.

4. COMPARATIVE STUDY

A performance comparisons of the 3 dB/45° patch coupler with rectangular ground slots (Design D) with other related works is summarized in Table 5.

Table 5. Performance comparison among the couplers (Design A, Design B, Design C and Design D) and other related works.

	Design A	**Design B**	**Design C**	**Design D (proposed)**	**[31]**	**[32]**	**[33]**
-10 dB bandwidth of $\|S_{11}\|$ (%)	14.15	28	26.02	28.90	21.40	22	10
1 dB amplitude imbalance bandwidth of $\|S_{31}\|$ (%)	16.62	36.46	33.90	39.14	24.50	42	30
5° phase imbalance bandwidth (%)	12.77	37.84	19.61	35.91	39.60	32	31
Electrical size ($\lambda_g \times \lambda_g$)	0.76×0.72	0.20×0.20	0.22×0.23	0.22×0.23	0.32×0.32	0.31×0.14	0.32×0.32

5. CONCLUSIONS

In this paper, a single-layered 3 dB/45° patch coupler with rectangular ground slots (Design D) is proposed. The inductive loading effect of cross slots in the proposed Design D coupler results in a significant size reduction of 45.72% compared to Design A coupler. The fractional bandwidths for -10 dB of $|S_{11}|$, -3 dB ± 1 dB of $|S_{31}|$ and 5° phase imbalance of output phase difference in Design D coupler are 28.90%, 39.14% and 35.91%, respectively. Moreover, the proposed Design D coupler provides bandwidth enhancements of 22.52% and 23.14% for -3 dB ± 1 dB coupling coefficient, $|S_{31}|$ and 45° ± 5° output phase difference compared to Design A coupler, respectively. The bandwidth of 45° ± 5° output phase difference in Design D coupler is increased by 16.3% owing to the presence of rectangular ground slots compared to Design C coupler. Therefore, the proposed 3 dB/45° patch coupler with rectangular ground slots (Design D) will be the attractive candidate in the future 5G beamforming networks such as Butler matrix without using additional phase shifters, which contributes to an overall size reduction while retaining reliable performance.

ACKNOWLEDGMENTS

This work was supported by the Ministry of Higher Education, Malaysia through the Fundamental Research Grant Scheme (203.PELECT.6071373).

REFERENCES

[1] I. A. Rumyancev and A. Korotkov, "Survey on Beamforming Techniques and Integrated Circuits for 5G

Systems," Proc. of the IEEE International Conference on Electrical Engineering and Photonics (EExPolytech), pp. 76-80, St. Petersburg, Russia, 2019.

[2] Federal Communications Commission, "Unlicensed Use of the 6 GHz Band, Notice of Proposed Rulemaking," Federal Registers, pp. 31997-32002, Washington, D.C, 2020.

[3] H. Nachouane, A. Najid, A. Tribak et al., "Broadband 4 × 4 Butler Matrix Using Wideband 90° Hybrid Couplers and Crossovers for Beamforming Networks," Proc. of the International Conference on Multimedia Computing and Systems (ICMCS), pp. 1444-1448, Marrakec, Morocco, 2014.

[4] D. N. A. Zaidel, S. K. A. Rahim and N. Seman, "4 × 4 Ultra-Wideband Butler Matrix for Switched Beam Array," Wireless Personal, vol. 82, no. 4, pp. 2471-2480, 2015.

[5] S. F. Ausordin, S. K. Abdul Rahim, N. Seman, R. Dewan and B. Sa'ad, "A c3.3ompact 4 × 4 Butler Matrix on Double-layer Substrate," Microwave and Optical Technology Letters, vol. 56, no. 1, pp. 223-229, 2013.

[6] R. Liang, Y. Zhang, W. Yan et al., "A Novel Design of Miniaturized Butler Matrix," Proc. of the 18th International Conference on Communication Technology (ICCT), pp. 560-563, Chongqing, China, 2018.

[7] K. Han, W. Li and Y. Liu, "Flexible Phase Difference of 4 × 4 Butler Matrix without Phase-shifters and Crossovers," International Journal of Antennas and Propagation, pp. 1-7, 2019.

[8] B. Li, Y. Chen, Z. Fu et al., "Substrate-guided Wave Optical True-time-delay Feeding Network for Phased-array Antenna Steering," Proc. of the International Society of Optics and Photonics (SPIE), pp. 256-265, San Jose, CA, United States, 2000.

[9] F. Casini, R. V. Gatti, L. Marcaccioli et al., "A Novel Design Method for Blass Matrix Beamforming Networks," Proc. of the 37th European Microwave Conference (EuMA), pp. 1512-1514, Munich, Germany, 2007.

[10] P. Chen, W. Hong, Z. Kuai and J. Xu, "A Double Layer Substrate Integrated Waveguide Blass Matrix for Beamforming Applications," IEEE Microwave and Wireless Components Letters, vol. 19, no. 6, pp. 374-376, 2009.

[11] W. Y. Lim and K. K. Chan, "Generation of Multiple Simultaneous Beams with a Modified Blass Matrix," Proc. of the Asia Pacific Microwave Conference (APMC), pp. 1557-1560, Singapore, 2009.

[12] T. Djerafi, N. J. G. Fonseca and K. Wu, "Broadband Substrate Integrated Waveguide 4 × 4 Nolen Matrix Based on Coupler Delay Compensation," IEEE Transactions on Microwave Theory and Techniques, vol. 59, no. 7, pp. 1740-1745, 2011.

[13] F. E. Fakoukakis and G. A. Kyriacou, "Novel Nolen Matrix Based Beamforming Networks for Series-fed Low SLL Multibeam Antennas," Progress in Electromagnetics Research, vol. 51, pp. 33-64, 2013.

[14] D. M. Pozar. Microwave Engineering, 4th Edn., New York: John Wiley & Sons, Inc., 2012.

[15] C. Gai, Y. Jiao and Y. Zhao, "Compact Dual-band Branch-line Coupler with Dual Transmission Lines," IEEE Microwave and Wireless Components Letters, vol. 26, no. 5, pp. 325-327, 2016.

[16] W. Feng, Y. Zhao, W. Che et al., "Dual-/Tri-Band Branch Line Couplers with High Power Division Isolation Using Coupled Lines," IEEE Transactions on Circuits and Systems II: Express Briefs, vol. 65, no. 4, pp. 461-465, 2018.

[17] L. Piazzon, P. Saad, P. Colantonio et al., "Branch-line Coupler Design Operating in Four Arbitrary Frequencies," IEEE Microwave and Wireless Components Letters, vol. 22, no. 2, pp. 67-69, 2012.

[18] A. M. Zaidi, M. T. Beg, B. K. Kanaujia et al. "A Dual Band Branch Line Coupler with Wide Frequency Ratio," IEEE Access, vol. 7, pp. 25046-25052, 2019.

[19] L. Xia, J. Li, B. A. Twumasi et al. "Planar Dual-band Branch-line Coupler with Large Frequency Ratio," IEEE Access, vol. 8, pp. 33188-33195, 2020.

[20] C. Gai, Y. C Jiao and Y. L. Zhao, "Arbitrary Power Division Quadrature Branch-line Coupler with Harmonic Suppression," Microwave and Optical Technology Letters, vol. 60, no. 1, pp. 256-260, 2017.

[21] H.-R. Ahn and M. M. Tentzeris, "Arbitrary Power-division Branch-line Hybrids for High-performance, Wideband and Selective Harmonic Suppressions from $2f_o$," IEEE Transactions on Microwave Theory and Techniques, vol. 67, no. 3, pp. 978-987, 2019.

[22] H.-J. Yoon and B.-W. Min, "Two Section Wideband 90° Hybrid Coupler Using Parallel-coupled Three-line," IEEE Microwave and Wireless Components Letters, vol. 27, no. 6, pp. 548-550, 2017.

[23] A. Bekasiewicz, "Miniaturized Dual-band Branch-line Coupler with Enhanced Bandwidth," Microwave and Optical Technology Letters, vol. 61, no. 6, pp. 1441–1444, 2019.

[24] U. Dilshad, C. Chen, X. Chen et al., "Broadband Quadrature Hybrid for Image Rejection in Millimeter-wave Receivers," Proc. of 16th International Bhurban Conference on Applied Sciences and Technology (IBCAST), pp. 975-978, Islamabad, Pakistan, 2019.

[25] J.-G. Chi and Y.-J. Kim, "A Compact Wideband Millimeter-wave Quadrature Hybrid Coupler Using Artificial Transmission Lines on a Glass Substrate," IEEE Microwave and Wireless Components Letters, vol. 30, no. 11, pp. 1037-1040, 2020.

[26] W. Yangsheng, H. Fuping and K. Dewu, "Design of Broadband Planar Magic-T Using 3-dB Branch-line Coupler and Phase Shifter," Proc. of the 3rd Asia-Pacific Conference on Antennas and Propagation, pp. 81-83, Harbin, China, 2014.

[27] D. Letavin, S. Shabunin and D. Trifonov, "Investigation of the Connection of Additional Stubs to the Phase Shifter Based on the Directional Coupler," Proc. of the 2019 Ural Symposium on Biomedical Engineering, Radioelectronics and Information Technology (USBEREIT), pp. 364-367, Yekaterinburg, Russia, 2019.

[28] S. S. Hesari and J. Bornemann, "Design of a SIW Variable Phase Shifter for Beam Steering Antenna Systems," Electronics, vol. 8, no. 9, pp. 1-14, 2019.

[29] W. Zhang, Z. Shen and S. J. Xuk, "A Compact Wideband Phase Shifter Using Slotted Substrate Integrated Waveguide," IEEE Microwave and Wireless Components Letters, vol. 29, no. 12, pp. 767-770, 2019.

[30] S. Liu and F. Xu, "Novel Substrate-Integrated Waveguide Phase Shifter and Its Application to Six-port Junction," IEEE Trans. on Microwave Theory and Techniques, vol. 67, no. 10, pp. 4167-4174, 2019.

[31] A. Singh and M. K. Mandal, "Arbitrary Coupling Arbitrary Phase Couplers with Improved Bandwidth," IET Microwaves, Antennas & Propagation, vol. 13, no. 6, pp. 748-755, 2019.

[32] Y. Wu, L. Jiao, Q. Xue et al., "A Universal Approach for Designing an Unequal Branch-line Coupler with Arbitrary Phase Differences and Input/Output Impedances," IEEE Transactions on Components, Packaging and Manufacturing Technology, vol. 7, no. 6, pp. 944-955, 2017.

[33] Q. He, C. Qi, C. Liu et al., "A Compact Arbitrary Power Division Coupler with Nonstandard Phase Difference," Journal of Electromagnetic Waves and Applications, vol. 32, no. 3, pp. 293-305, 2017.

[34] S. A. Babale et al., "Single Layered 4 × 4 Butler Matrix without Phase Shifters and Crossovers," IEEE Access, vol. 6, pp. 77289-77298, 2018.

[35] Y. -L. Li, Q. S. Liu, S. Sun and S. S. Gao, "A Miniaturised Butler Matrix Based on Patch Hybrid Couplers with Cross Slots," Proc. of the IEEE Antennas and Propagation Society International Symposium (APSURSI), pp. 2145-2146, Orlando, FL, USA, 2013.

[36] M. Moubadir, H. Aziz, N. A. Touhami and A. Mohamed, "A Miniaturized Branch-line Hybrid Coupler Microstrip for Long Term Evolution Applications," Procedia Manufacturing, vol. 22, pp. 491–497, 2018.

[37] P. Upadhyay, V. Sharma and R. Sharma, "Design of Microstrip Patch Antenna Array for WLAN Application," Int. J. of Engineering and Innovative Technology (IJEIT), vol. 2, no. 1, pp. 295-297, 2012.

[38] Y. S. Wong, S. Y. Zheng and W. S. Chan, "Quasi-arbitrary Phase-difference Hybrid Coupler," IEEE Transactions on Microwave Theory and Techniques, vol. 60, no. 6, pp. 1530-1539, 2012.

[39] Y. Wu, J. Shen and Y. Liu, "Comments on “Quasi-arbitrary Phase-difference Hybrid Coupler”," IEEE Transactions on Microwave Theory and Techniques, vol. 61, no. 4, pp. 1725-1727, 2013.

[40] S. Sun and L. Zhu, "Miniaturised Patch Hybrid Couplers Using Asymmetrically Loaded Cross Slots," IET Microwaves, Antennas & Propagation, vol. 4, no. 9, pp. 1427-1433, 2010.

ملخص البحث:

في هذا البحث، يتمّ اقتراح نظام ربطٍ أحادي الطّبقة (3 ديسيبل/45 درجة) يرمز اليه بالتّصميم D لشبكات تشكيل الشُّعاع من الجيل الخامس (5G) باستخدام بُنيةٍ مشقوقة عرْضياً في هيئة شقوقٍ على شكل كُرتيْن بينهما قضيب، وأروماتٍ وصْلٍ محمَّلة، وأثلام، وشقوق أساسية مستطيلة. ويمتلك نظام الرّبط المقترح (التّصميم D) القدرة على إلغاء الحاجة الى مُزيحات طوْر إضافية بزاوية 45 درجة في شبكات تشكيل الشُّعاع مثل مصفوفة بَتْلَر، الأمر الذي يمثّل الإسهام الرئيسي لهذا البحث، وبخاصّةٍ فيما يتعلّق بتقليل الحجم وتحسينات عَرْض النّطاق. ويؤدي التّصميم D المقترح الى تحقيق نطاقاتٍ جزئيّة قدرها 28.9% و 39.14% و 35.91% لِـ (-10 ديسيبل) بالنّسبة الى |S11|، و (-3 ديسيبل± 1 ديسيبل) بالنسبة الى |S31|، و 5 درجات من عدم الإتّزان بالنّسبة الى فَرْق الطّوْر في المخرج. وتبلغ التّحسينات في عَرْض النّطاق (-3 ديسيبل±1ديسيبل) بالنسبة الى معامل الربْط S31 و (45±5 درجات) بالنّسبة الى فرق الطّوْر في المخرج التي يحقّقها النّظام المقترح (التصميم D) 22.52% و 23.14% مقارنةً بالتصميم A، على الترتيب. ويتحقق تحسين عَرْض النّطاق لفرق الطّوْر في المخرج (45±5 درجات) بحيث يزداد بنسبة 16.3% بسبب وجود الشُّقوق الأساسية المستطيلة في التّصميم D المقترح مقارنةً بنظام الرّبط للتّصميم C. يبلغ حجم التّصميم المقترح (التصميم D) ($0.23\ \lambda_g\ x\ 0.22\ \lambda_g$) ويعني ذلك أنّ الحجم الكهربائي لنظام الربط المقترح (التصميم D) هو أقل بنسبة (45.72%) مقارنةً بنظام الرّبط ذي التّصميم A.